Novel Cellulose Derivatives. I. Liquid Crystal Phase Formation in Tri-*O*-α-Naphthylmethyl Cellulose Solutions

VIPUL DAVÉ, CHARLES E. FRAZIER, and WOLFGANG G. GLASSER*

Department of Wood Science and Forest Products, and Biobased Materials Center, Polymer Materials and Interfaces Laboratory, Virginia Polytechnic Institute and State University, Blacksburg, Virginia 24061

SYNOPSIS

Tri-*O*-α-naphthylmethyl cellulose was prepared by homogeneous phase reaction using SO_2–diethylamine (DEA)–dimethyl sulfoxide (DMSO) as the solvent system. Observations made by dynamic mechanical spectrometry and by cross-polarized optical microscopy revealed liquid crystalline behavior for the concentrated solutions of tri-*O*-α-naphthylmethyl cellulose in dimethylacetamide (DMAc). Experimental and calculated (predicted) critical volume fraction of the derivative, V_p^c, did not show agreement. It is determined that V_p^c is affected by bulky substituents on the cellulose backbone to some extent. © 1993 John Wiley & Sons, Inc.

INTRODUCTION

In recent years, numerous publications have appeared pertaining to the liquid crystalline behavior of concentrated solutions of cellulose and cellulose derivatives in different solvent systems. Our research efforts are directed toward understanding the effects of different types of side chain substituents on the onset of liquid crystallinity in cellulose derivative solutions. We have established in our earlier investigations[1,2] that solution anisotropy can be reached at lower concentrations in cellulose esters with large and bulky substituents compared to smaller ones. The general trend was that the experimental critical volume fraction (V_p^c) values were lower than the calculated (predicted) values from Flory's theory. We gained further insights on the effects of side chain substituents on liquid crystalline behavior by extending our investigations to homogeneously prepared cellulose ether derivatives.

The objective of the present study is to examine the lyotropic liquid crystalline behavior of tri-*O*-α-naphthylmethyl cellulose in dimethylacetamide (DMAc) in relation to the bulky naphthyl groups on the cellulose backbone. En route, we would also like to supply a basic spectroscopic characterization of this relatively rare cellulose derivative. By employing simple two-dimensional, and polarization transfer pulse sequences on this and related polymers, we wish merely to achieve a more complete characterization of the polymer.

EXPERIMENTAL

Preparation of Tri-*O*-α-Naphthylmethyl Cellulose

Tri-*O*-α-Naphthylmethyl cellulose was prepared by scaling up the procedure described by Isogai et al.[3,4] Whatman, CF-11, cellulose, 10 g, was dissolved in a nonaqueous SO_2–diethylamine (DEA)–dimethyl sulfoxide (DMSO) solvent mixture, and powdered sodium hydroxide, 15 equiv./OH, was added to the solution.[3,4] However, the following conditions were different from Isogai's methodology. All reactions were carried out under N_2, and were then ended by pouring the cooled reaction mixture into 4 L of distilled water. The polymer formed a stable emulsion that settled nicely to the bottom of the beaker. The liquid layer was decanted, and more distilled water was added with vigorous stirring. This procedure was repeated until the liquid layer was colorless. The water was decanted again, and 3 L of methanol were added to cause precipitation of the polymer. The product was filtered and extracted with methanol in

* To whom correspondence should be addressed.

Journal of Applied Polymer Science, Vol. 49, 1671–1678 (1993)
 CCC 0021-8995/93/091671-08

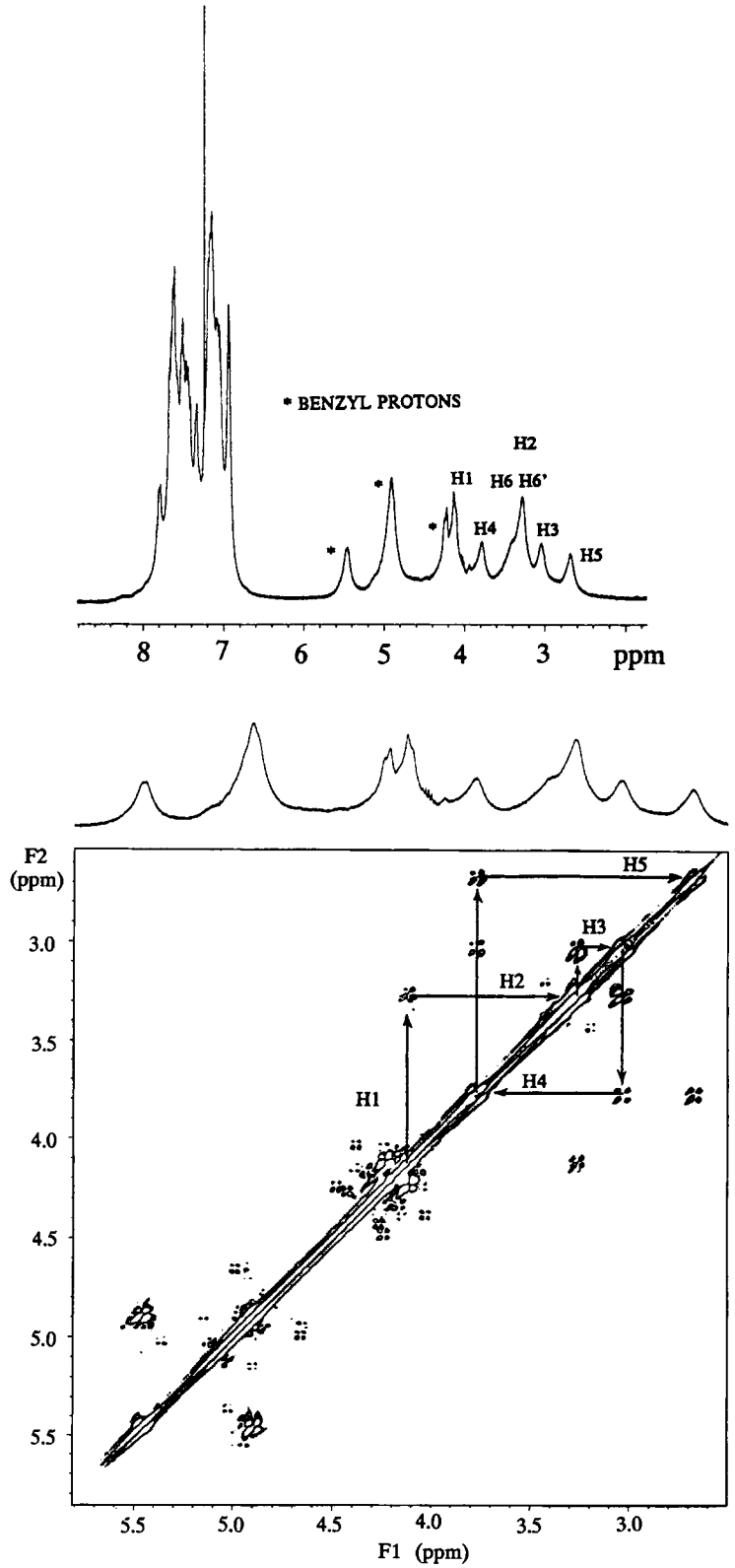

Figure 1 (a) Proton NMR spectrum of tri-*O*-α-naphthylmethyl cellulose. (b) Two dimensional COSY (DQCOSY) spectrum of tri-*O*-α-naphthylmethyl cellulose. (c) Chemical structure of tri-*O*-α-naphthylmethyl cellulose.

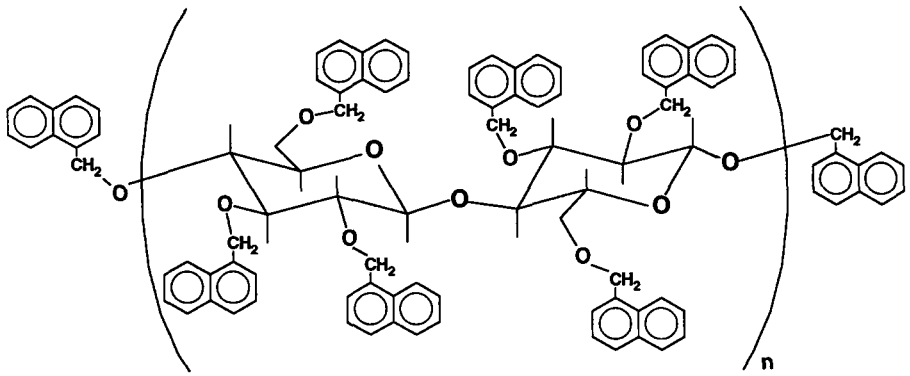

Figure 1 *(Continued from the previous page)*

a soxhlet for at least 72 h. The color of the polymer remained bright orange even after additional acetone extraction for 48 h. The polymer was dried, dissolved in tetrahydrofuran (THF), and centrifuged to remove any insoluble material. The supernatant was concentrated and then precipitated into methanol. The polymer was finally dried under high vacuum for 24 h. Yields were typically 70–80% of the theoretical value. The product was soluble in THF, chloroform, dioxane, and dimethylacetamide, and insoluble in methanol, ethanol, and acetone.

Determination of Molecular Weights

A solution of tri-*O*-α-naphthylmethyl cellulose was prepared in HPLC-grade THF. Gel permeation chromatography was used, where THF was pumped with a Waters 510 chromatography pump into a series of 3, Waters, Ultrastyragel columns, with pore sizes of 10^3, 10^4, and 10^6 Å. Detection was with a Waters 410 refractometer, in series with a Model 100 differential viscosity detector (Viscotek Corp.). The columns were heated to 40°C in an Eldex column heater, and both detectors were also heated to 40°C. THF was freshly degassed, and always stored under a helium atmosphere during use. Narrow polydispersity, polystyrene standards from Polymer Laboratories were used to establish a universal calibration.

NMR Spectroscopy

All NMR spectra were collected on a Varian Unity 400 instrument at 400 and 100 MHz for proton and carbon nuclei, respectively. Samples for proton NMR were prepared in 5-mm NMR tubes by dissolving 25–40 mg of sample in about 0.5–0.7 mL of deuterated chloroform. Samples for carbon NMR were prepared in 10-mm NMR tubes by dissolving 150–200 mg of sample in about 2.5–3 mL of deuterated chloroform. A standard Double Quantum filtered COSY, DQCOSY, pulse sequence was run at 40°C.

Preparation of Concentrated Solutions

A complete range of tri-*O*-α-naphthylmethyl cellulose solutions [5–50% (w/w)] was prepared by mechanically mixing known weights of naphthyl cellulose with DMAc at ambient temperature. The solutions were allowed to equilibrate for 2 weeks prior to analysis.

Viscosity Measurements

Viscosity measurements of the solutions below 30% (w/w) concentration were made at 25°C using a Wells–Brookfield Cone/Plate Viscometer at different rotational speeds. Rheometrics Mechanical Spectrometer (RMS 800) was used to determine the rheological properties of 30% (w/w) and higher concentrated solutions. The solutions were placed in a parallel-disk geometry. The dynamic mechanical properties were measured at 26°C using a strain amplitude of 25%. This strain level was selected on the basis of a "strain sweep" experiment (i.e., measuring dynamic viscosity at variable strain amplitudes) that ascertained that the solutions were within the linear range of the viscoelastic response. All frequency sweep tests were conducted using constant strain (25%) and variable concentration. The frequency ranged from 0.1 to 100 rad/s.

Polarized Optical Microscopy

Microscopy experiments were performed on a Zeiss Axioplan Universal Microscope. Small portions of solution were placed between microscope slide and

Table I Molecular, Chemical, and Thermal Characteristics of Tri-*O*-α-Naphthylmethyl Cellulose

$\langle M_n \rangle$, g/mol (10^{-3})	43
$\langle M_w \rangle$, g/mol (10^{-3})	150
$\langle M_w \rangle / \langle M_n \rangle$	3.5
DP_n	74
Degree of substitution	3.0
MHS-constant, a	0.64
Log K	−3.4
Intrinsic viscosity [η] (dL/g)	0.64
Melting temperature (°C)	94
Heat capacity (J/g)	64.7

cover slip, and this was examined for birefringence between the cross polarizers of the microscope at room temperature.

RESULTS AND DISCUSSION

Structure Characterization

The molecular, chemical, and thermal characteristics of tri-*O*-α-naphthylmethyl cellulose are summarized in Table I. The DP_n of unmodified Whatman cellulose (parent polymer) was about 220, but that of the cellulose ether derivative was reduced to 74. Previous experience has shown that the combination of powdered alkali, DMSO, and especially SO_2, is extremely degradative to the cellulose backbone. Atmospheric oxygen was always excluded, and therefore was not involved in this degradation.

Table II Peak Assignments of Proton and Carbon Signals of Tri-*O*-α-Naphthylmethyl Cellulose

	Anhydroglucose Unit (ppm)	Benzyl (ppm)
H1	4.12	
H2	3.28	
H3	3.04	
H4	3.78	
H5	2.68	
H6	3.40	
H6′	3.20	
Benzyl protons		5.19, 4.91, 4.2
C1	101.9	
C2	81.2	
C3	82.4	
C4	ca. 77	
C5	74	
C6	67.4	
Benzyl carbons		72.3, 72.2, 71.4

The backbone proton resonances have been assigned [Fig. 1(a)] using the two-dimensional, DQCOSY, pulse sequence [Fig. 1(b)]. For reference, the chemical structure of tri-*O*-α-naphthylmethyl cellulose is shown in Figure 1(c). Table II lists the

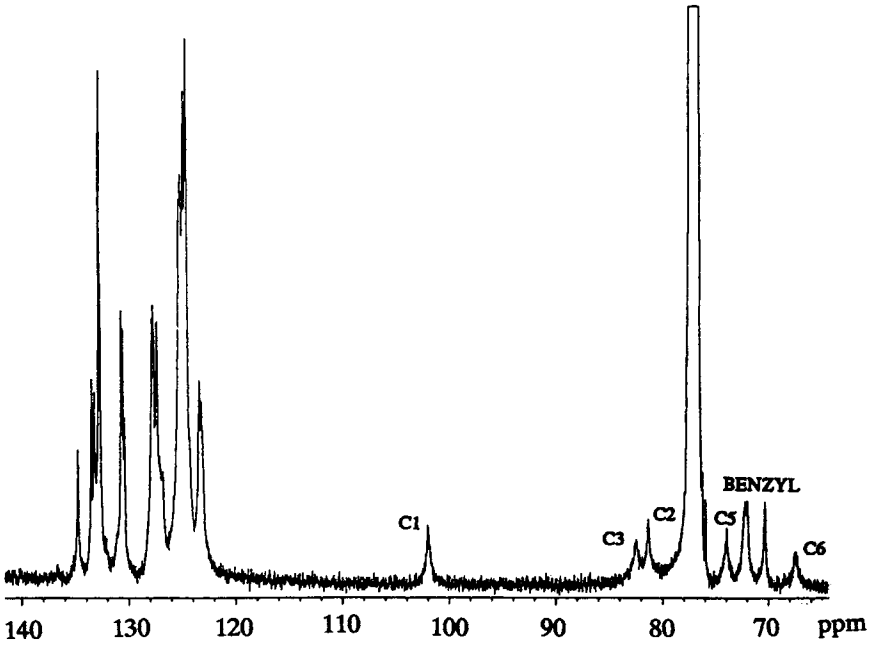

Figure 2 ^{13}C NMR spectrum of tri-*O*-α-naphthylmethyl cellulose.

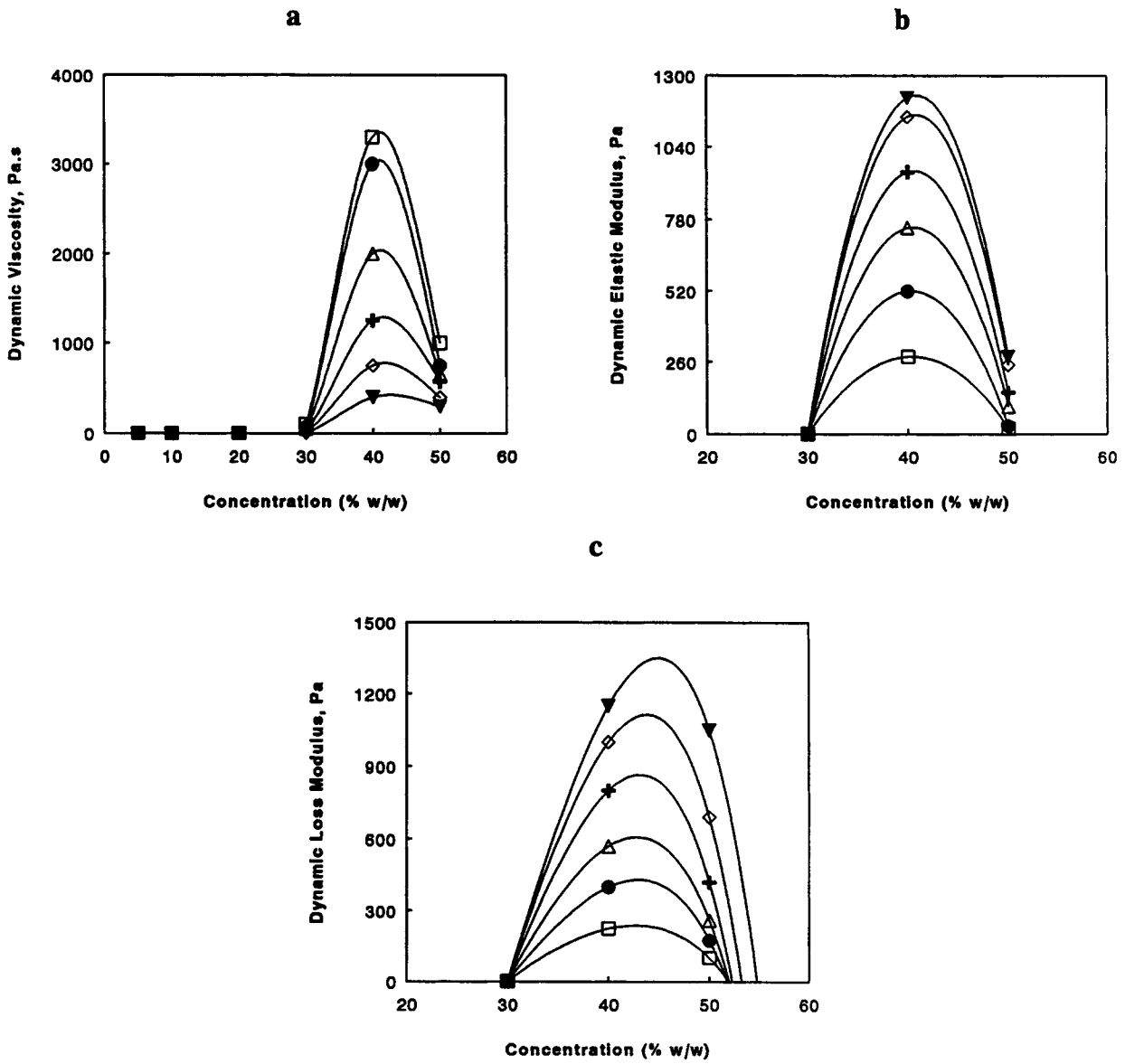

Figure 3 (a) Dynamic viscosity; (b) dynamic elastic modulus; and (c) dynamic loss modulus vs. concentration of tri-*O*-α-naphthylmethyl cellulose solutions at different frequencies. All graphs: 0.1 rad/s (□); 0.2 rad/s (●); 0.5 rad/s (△); 1.0 rad/s (+); 2.0 rad/s (◇); 5.0 rad/s (▼).

peak assignments of the backbone proton resonances as indicated in Figure 1(a). The DQCOSY pulse sequence establishes the relative proximity of neighboring protons by detecting the coupling that occurs between geminal and vicinal hydrogens. Couplings, or correlations, appear as signals removed from the main diagonal and on both sides of the diagonal, whereas the individual signals appear on the diagonal, as in a one-dimensional spectrum [Fig. 1(b)]. If an off-diagonal coupling is equidistant from two, on-diagonal signals, a perfect right angle is formed, and those connected signals represent nearest neighbors. Previous work with benzylated cellulose derivatives has proven that the signal at 4.12 ppm arises from the proton at position 1 [Fig. 1(c)].[5] By following the correlations as revealed in Figure 1(b), one can assign the remaining signals by starting the analysis at position 1, δ = 4.12 ppm. Notice that the correlation between protons at positions 5 and 6 is not observed for reasons beyond the scope of this discussion. However, a weak correlation is observed between signals at 3.2 and 3.4

ppm. These two signals are assigned, by default, as the geminal protons at position 6.

Appropriately, however, the 6 position protons have also been assigned by heteronuclear correlation, HETCOR, to carbon 6 of the ^{13}C NMR spectrum (Fig. 2). The HETCOR experiment establishes proton–carbon connectivity. While not performed on tri-*O*-α-naphthylmethyl cellulose, we have performed the HETCOR on similar arylmethyl cellulose derivatives.[5] We found little variation in carbon resonances among arylmethyl celluloses, and therefore base these carbon assignments on previous experiments with benzylated cellulose.[5] The resulting carbon assignments (Table II) were checked using Distortionless Enhancement Polarization Transfer (DEPT). DEPT distinguishes methyl, methylene, and methine carbons, and therefore supported the assignment of methylene carbon 6 and the 3 methylene benzyl carbons (Fig. 2).

Liquid Crystalline Behavior

The relationship between the dynamic shear viscosity and concentration of naphthylmethyl cellulose was studied at different frequencies (Fig. 3). The viscosity increases with concentration up to a maximum before declining with further increase in concentration. At the point of maximum viscosity, the polymer solution reaches a critical concentration beyond which it becomes birefringent. This marks the commencement of liquid crystallinity. In the case of naphthylmethyl cellulose, the point of maximum viscosity is at 41% (w/w) concentration, and we define it to be the critical concentration (weight fraction) value. Such an anomalous viscosity behavior is typical for liquid crystalline solutions, and this has been shown previously for cellulose acetate,[6,7] ethyl cellulose,[8] hydroxypropyl cellulose,[7,9] and cellulose triacetate.[10] This change in viscosity is caused by a change in the structure of the solution. As the concentration rises, the size and density of the ordered clusters in an isotropic matrix increases.[11] The energy dissipated by these clusters during flow is less than the sum of the energies dissipated by each individual molecule; hence the viscosity decreases with concentration.

The dynamic elastic modulus (G') behaves similarly to the dynamic viscosity; that is, after the solution becomes anisotropic, G' declines [Fig. 3(b)]. As with any viscoelastic material, G' and G'' rise with frequency.

The polarized optical micrographs of 40 and 50% (w/w) concentrations of the derivative show the transition from biphasic [Fig. 4(a)] to completely anisotropic solution, respectively [Fig. 4(b)]. In the case of polymers, a biphasic region (isotropic and liquid crystal phases) is routinely observed because of polydispersity, impurities, or chain imperfections. There is a good correlation between dynamic viscosity measurements and polarized optical microscopy results that confirm that the onset of liquid crystalline behavior in naphthylmethyl cellulose in DMAc is at 41% (w/w). This is the first report of lyotropic mesophase formation of naphthylmethyl cellulose.

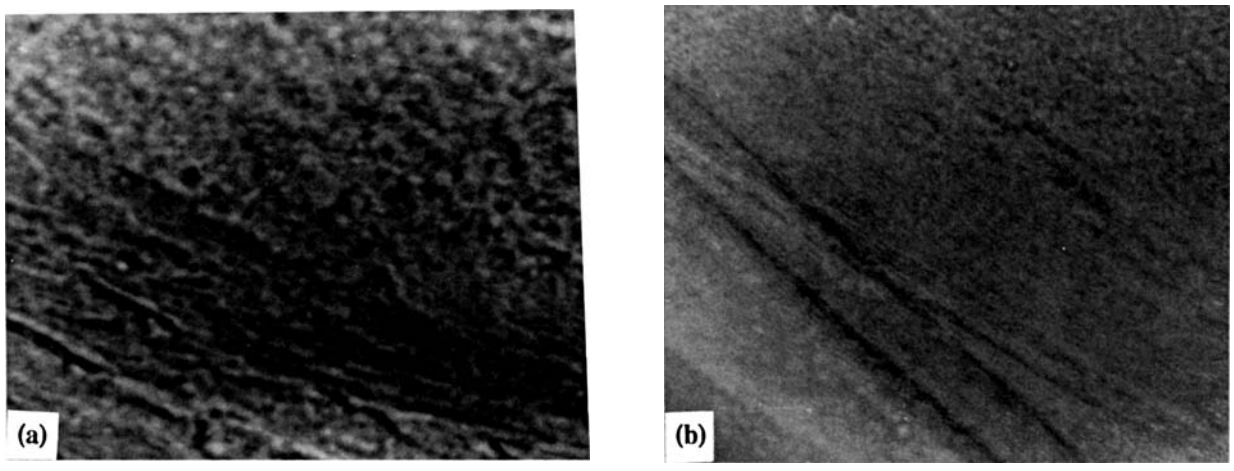

Figure 4 Polarized optical micrographs of tri-*O*-α-naphthylmethyl cellulose solutions (a) 40% (w/w); (b) 50% (w/w).

Table III Theoretical Values of Molecular Parameters for Cellulose Derivatives

Cell. Deriv.	M_u (g/mol)	d (Å)	l_k (Å)	q (Å)	x_k	V_p^c, Th.	V_p^c, Expt.
CA[a]	264.5	8.06	207.7	103.85	25.77	0.29	0.38
CAB-1	303.3	8.98	207.7	103.85	23.13	0.32	0.34
CAB-2	326.2	9.32	207.7	103.85	22.29	0.33	0.32
CAB-3	354.1	9.71	207.7	103.85	21.40	0.34	0.29
NC[b]	582	12.68	192.3	96.15	15.16	0.46	0.35

[a] Cellulose acetate and cellulose acetate butyrates (CA, CAB-1, CAB-2, CAB-3): values obtained from reference 1.
[b] Tri-*O*-α-naphthylmethyl cellulose: values from Appendix A.

Tri-*O*-α-naphthylmethyl cellulose melted at 94°C but did not exhibit thermotropic liquid crystalline behavior. However, thermotropic liquid crystallinity was previously reported for this particular cellulose ether derivative, with crystal to smectic, smectic to nematic, and nematic to isotropic transitions at 140°C, 160°C, and 200°C, respectively.[12]

The MHS-constant, a, of tri-*O*-α-naphthylmethyl cellulose was 0.64 (Table I), which curiously represents a flexible polymer chain. Values of a for cellulose and cellulose derivatives are typically in the range of 0.9–1.0 and indicate that they are semirigid polymers. In spite of the low a value, the derivative in our study formed lyotropic solutions at high concentrations. This means that stiffness of the chain is much higher than predicted by the MHS equation, and liquid crystal formation is caused by intramolecular and intermolecular effects.

The experimental volume fraction, V_p^c (0.35), is lower than the calculated value (0.46) (see Table III and Appendix A for calculations) for tri-*O*-α-naphthylmethyl cellulose.

The critical volume fraction was not greatly affected by molecular weight for hydroxypropyl cellulose (HPC)[15] and (acetoxypropyl) cellulose (APC)[16] in DMAc. Therefore, we cautiously compare the experimental results obtained in this study with our previous work on cellulose esters with different substituents,[1] even though the molecular weights differ to some extent. When considering the relationship between the experimental and predicted values of V_p^c and molecular weight of the repeat unit, M_u, for cellulose esters (see Table III) and tri-*O*-α-naphthylmethyl cellulose, the experimental values of V_p^c, in general, are lower than the theoretical values for all the cellulose derivatives (Fig. 5). This difference may be caused by secondary intermolecular interactions, intramolecular steric effects, and/or polydispersity that are neglected in the theoretical calculations. During the study of liquid crystalline solutions of HPC in DMAc, complete agreement between the experimental and calculated values of V_p^c required the assumption of a small degree of soft interaction.[15-17]

V_p^c is indeed related to M_u, but in a more complex way than is expressed in Flory's model.[17]

CONCLUSIONS

1. Tri-*O*-α-naphthylmethyl cellulose was successfully prepared by employing a nonaqueous cellulose solvent, SO_2–DEA–DMSO.
2. Tri-*O*-α-naphthylmethyl cellulose solution in DMAc exhibited liquid crystalline behavior as observed by viscosity measurements and cross polarized optical microscopy results.
3. Flory's theory[17] overestimates V_p^c. Although molecular weight of the repeat unit of cellulose derivatives does seem to influence V_p^c to

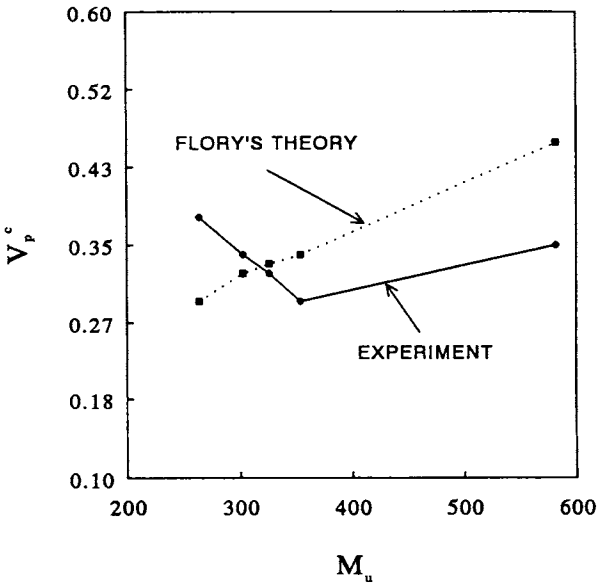

Figure 5 Experimental and theoretical relationship between critical volume fraction of cellulose derivatives V_p^c, and molecular weight of the repeating unit, M_n.

some degree, other factors, especially intermolecular interactions and polydisperisty, seem to be of importance as well.

We appreciate the support of this research by the National Science Foundation Science and Technology Center for High Performance Polymeric Adhesives and Composites at Virginia Tech under contract DMR8809714.

APPENDIX A

Equations used for theoretical calculations are taken from Flory.[13]

1. Calculation of molecular weight of repeat unit, M_u:

$$M_u = 162 + 3(11 \times 12 + 9) - 3$$
$$= 582 \text{ g/mol.}$$

2. Calculation of chain diameter, d:

$$d = (M_u/N_A\rho l_u)^{1/2}$$
$$d = (582/6.02 \times 10^{23} \times 1.17 \times 10^{-24} \times 5.14)^{1/2} = 12.68 \text{ Å.}$$

3. Calculation of Kuhn segment length, l_k: $l_k = \langle r_2 \rangle_o / n l_u$. From light scattering[14] $\langle r^2 \rangle_o / n = 1000$ Å^2 for cellulose ethers.

$$l_k = 1000/5.14 = 192.30 \text{ Å.}$$

4. Calculation of persistence length, q:

$$q = l_k/2$$
$$q = 192.30/2 = 96.15 \text{ Å.}$$

5. Calculation of aspect ratio, X_k:

$$X_k = 2q/d$$
$$X_k = 2 \times 96.15/12.68 = 15.16.$$

6. Calculation of critical volume fraction, V_p^c:

$$V_p^c = 8/X_k(1 - 2/X_k)$$
$$V_p^c = 8/15.16\ (1 - 2/15.16) = 0.46.$$

REFERENCES

1. V. Davé and W. G. Glasser, in *Viscoelasticity of Biomaterials,* ACS Symp. Ser. No. 489, W. G. Glasser and H. Hatakeyama, Eds., 1992, pp. 144–166.
2. V. Davé and W. G. Glasser, *J. Appl. Polym. Sci.,* to appear.
3. A. Isogai, A. Ishizu, and J. Nakano, *J. Appl. Polym. Sci.,* **29,** 2097–2109 (1984).
4. A. Isogai, A. Ishizu, and J. Nakano, *J. Appl. Polym. Sci.,* **29,** 3873–3882 (1984).
5. C. E. Frazier and W. G. Glasser, to appear.
6. S. Dayan, P. Maissa, M. J. Vellutini, and P. Sixou, *J. Polym. Sci., Polym. Lett. Ed.,* **20,** 33–43 (1982).
7. S. Dayan, J. M. Gilli, and P. Sixou, *J. Appl. Polym. Sci.,* **28,** 1527–1534 (1983).
8. S. Suto, *J. Polym. Sci., Polym. Phys. Ed.,* **22,** 637–646 (1984).
9. P. Navard and J. M. Haudin, *J. Polym. Sci.: Polym. Phys. Ed.,* **35,** 189–201 (1986).
10. Y. K. Hong, D. E. Hawkinson, E. Kohout, A. Garrard, R. E. Fornes, and R. D. Gilbert in *Polymer Association Structure,* Chap. 12, M. A. El-Nokaly, Ed., ACS Symp. Ser. No. 384, 1989, pp. 184–203.
11. D. G. Baird, *J. Rheology,* **24,** 465–482 (1980).
12. A. Isogai, A. Ishizu, and J. Nakano, *J. Appl. Polym. Sci.,* **30,** 345–353 (1985).
13. P. J. Flory, *Adv. in Polym. Sci.,* **59,** 2–36 (1984).
14. M. G. Wirick and M. H. Waldman, *J. Appl. Polym. Sci.,* **14,** 579 (1970).
15. G. Conio, E. Bianchi, A. Ciferri, A. Tealdi, and M. A. Aden, *Macromolecules,* **16,** 1264–1270 (1983).
16. G. V. Laivins, P. Sixou, and D. G. Gray, *J. Polym. Sci., B Polym. Phys.,* **24,** 2779–2792 (1986).
17. M. A. Aden, E. Bianchi, A. Ciferri, G. Conio, and A. Tealdi, *Macromolecules,* **17,** 2010–2015 (1984).

Received September 11, 1992
Accepted December 21, 1992